Biochimica et Biophysica Acta 1777 (2008) 525–531

Contents lists available at ScienceDirect

Biochimica et Biophysica Acta

journal homepage: www.elsevier.com/locate/bbabio

Molecular origin of the pH dependence of tyrosine D oxidation kinetics and radical stability in photosystem II

Rainer Hienerwadel [a,b,c,*], Bruce A. Diner [d], Catherine Berthomieu [e,f,g]

[a] Aix-Marseille Université, Laboratoire de Génétique et de Biophysique des Plantes, F-13009, France
[b] CNRS, UMR Biol Veget & Microbiol Environ, Marseille, F-13009, France
[c] CEA, DSV, IBEB, Marseille, F-13009, France
[d] CR&D, Experimental Station, E. I. du Pont de Nemours & Co., Wilmington, DE, 19880-0173, USA
[e] CEA, DSV, IBEB, Laboratoire des Interactions Protéine Métal, Saint-Paul-lez-Durance, F-13108, France
[f] CNRS, UMR Biol Veget & Microbiol Environ, Saint-Paul-lez-Durance, F-13108, France
[g] Aix-Marseille Université, Saint-Paul-lez-Durance, F-13108, France

ARTICLE INFO

Article history:
Received 13 February 2008
Received in revised form 1 April 2008
Accepted 2 April 2008
Available online 10 April 2008

Keywords:
FTIR
Photosystem II
Redox-active tyrosine
Synechocystis PCC 6803
Tyrosyl radical
TyrD

ABSTRACT

A role for redox-active tyrosines has been demonstrated in many important biological processes, including water oxidation carried out by photosystem II (PSII) of oxygenic photosynthesis. The rates of tyrosine oxidation and reduction and the Tyr·/Tyr reduction potential are undoubtedly controlled by the immediate environment of the tyrosine, with the coupling of electron and proton transfer, a critical component of the kinetic and redox behavior. It has been demonstrated by Faller et al. that the rate of oxidation of tyrosine D (Tyr_D) at room temperature and the extent of Tyr_D oxidation at cryogenic temperatures, following flash excitation, dramatically increase as a function of pH with a pK_a of ≈7.6 [Faller et al. 2001 Proc. Natl. Acad. Sci. USA 98, 14368–14373; Faller et al. 2001 Biochemistry 41, 12914–12920]. In this work, we investigated, using FTIR difference spectroscopy, the mechanistic reasons behind this large pH dependence. These studies were carried out on Mn-depleted PSII core complexes isolated from *Synechocystis* sp. PCC 6803, WT unlabeled and labeled with $^{13}C_6$-, or $^{13}C_1$(4)-labeled tyrosine, as well as on the D2-Gln164Glu mutant. The main conclusions of this work are that the pH-induced changes involve the reduced Tyr_D state and not the oxidized Tyr_D state and that Tyr_D does not exist in the tyrosinate form between pH 6 and 10. We can also exclude a change in the protonation state of D2-His189 as being responsible for the large pH dependence of Tyr_D oxidation. Indeed, our data are consistent with D2-His189 being neutral both in the Tyr_D and Tyr_D states in the whole pH6-10 range. We show that the interactions between reduced Tyr_D and D2-His189 are modulated by the pH. At pH greater than 7.5, the ν(CO) mode frequency of Tyr_D indicates that Tyr_D is involved in a strong hydrogen bond, as a hydrogen bond donor only, in a fraction of the PSII centers. At pH below 7.5, the hydrogen-bonding interaction formed by Tyr_D is weaker and Tyr_D could be also involved as a hydrogen bond acceptor, according to calculations performed by Takahashi and Noguchi [J. Phys. Chem. B 2007 111, 13833–13844]. The involvement of Tyr_D in this strong hydrogen-bonding interaction correlates with the ability to oxidize Tyr_D at cryogenic temperatures and rapidly at room temperature. A strong hydrogen-bonding interaction is also observed at pH 6 in the D2-Gln164Glu mutant, showing that the residue at position D2-164 regulates the properties of Tyr_D. The IR data point to the role of a protonatable group(s) (with a pK_a of ≈7) other than D2-His189 and Tyr_D, in modifying the characteristics of the Tyr_D hydrogen-bonding interactions, and hence its oxidation properties. It remains to be determined whether the strong hydrogen-bonding interaction involves D2-His189 and if Tyr_D oxidation involves the same proton transfer route at low and at high pH.

1. Introduction

Redox-active tyrosines play essential roles in many biologically important processes [1]. Their presence has been demonstrated in key enzymes such as ribonucleotide reductase [2], involved in the synthesis of deoxyribonucleotides, and in the bioenergetic complexes, photosystem II (PSII) [3] and cytochrome oxidase [4]. Tyrosine radicals have also been shown to be present in catalases, peroxidases, and catalase-peroxidases having a protoporphyrin at the active site [5–7] and in the DNA photolyase from *Anacystis nidulans*, involved in DNA repair [8]. The diverse functions and properties of these redox-active tyrosines imply that the redox properties, reactivity, and radical stability are regulated by the protein environment. Features of that environment that are likely to influence tyrosine radical behavior are

Abbreviations: PS II, photosystem II; Tyr_Z and Tyr_D, the two redox-active tyrosines of photosystem II on the D1 (D1-160) and D2 (D2-160, *Synechocystis* sp. *PCC 6803* numbering) polypeptides, respectively

* Corresponding author. Aix-Marseille Université, Laboratoire de Génétique et de Biophysique des Plantes, F-13009, France. Tel.: +33 4 91 82 94 11; fax: +33 4 91 82 94 12.
E-mail address: rainer.hienerwadel@univmed.fr (R. Hienerwadel).

0005-2728/$ – see front matter © 2008 Elsevier B.V. All rights reserved.
doi:10.1016/j.bbabio.2008.04.004

the distribution of charges in the vicinity of the radical and the hydrogen-bonding interactions with proton accepting base(s), which control the proton transfer reactions accompanying Tyr oxidation.

Two strictly conserved redox-active tyrosines are present in PSII, at homologous positions on the D1 and D2 polypeptides which form the dimeric core of the PSII reaction center. Both are oxidized by the oxidized form of the special pair chlorophylls, P_{680}^{+}. Whereas tyrosine Z (Tyr_Z) on the D1 polypeptide is a highly reactive and oxidizing intermediate involved in water oxidation, the homologous tyrosine D (Tyr_D) on the D2 polypeptide forms a radical that is stable for hours in the dark at pH 6 [reviewed in 9]. It has been shown, however, that under special circumstances Tyr_D can be involved in the oxidation or reduction of certain states of the Mn cluster involved in water oxidation [reviewed in 10] and that the presence of Tyr_D facilitates the photoassembly of the Mn cluster [11].

Spectroscopic studies, mutagenesis experiments and the recently published X-ray crystallographic structures of PSII have shown that Tyr_D forms a hydrogen-bonding interaction with D2-His189 [9,12–17]. Several of the studies have focused on the role of this interaction on the properties of $Tyr_D^{\cdot}$. The pH has a large influence on the kinetics of formation of $Tyr_D^{\cdot}$ and its stability in Mn-depleted PSII. $Tyr_D^{\cdot}$ is stable for hours at pH 6, but decays in tens of minutes in the dark at pH 8 [18]. Using a genetically engineered Tyr_Z-less strain of *Synechocystis* sp. PCC 6803, Faller et al. [19] showed that at room temperature, the oxidation of Tyr_D by P_{680}^{+} is rapid at pH 8.5 ($t_{1/2} \approx 190$ ns) and comparable or even faster than that of Tyr_Z, while at pH 6.5, the rate of Tyr_D oxidation is in the ms range, and much slower than that of Tyr_Z ($t_{1/2} \approx 2$–20 μs). This drastic effect of pH on the kinetics of Tyr_D oxidation titrates with an apparent pK_a of 7.7 [19], suggesting a pH-dependent change of protonation state of either Tyr_D itself or its neighboring residues.

Tyr_D oxidation by P_{680}^{+} was also detected at 15 K for PSII core complexes at pH > 8 [20]. This phenomenon was observed in about 75% of the PSII centers in *Synechocystis* sp. 6803 and in about 50% of the centers in Mn-depleted PSII from spinach. Two mechanisms were proposed to explain the unexpected ability of Tyr_D to undergo, at elevated pH, oxidation at cryogenic temperatures: either 1) proton tunneling along the hydrogen bond between Tyr_D and the imidazole ring of D2-His189 to form a $Tyr_D^{\cdot}$-$HisH^{+}$ pair, or 2) the presence of a deprotonated Tyr_D^{-} (tyrosinate) prior to oxidation, leading to a pure electron transfer to form the $Tyr_D^{\cdot}$ – His pair upon oxidation by P_{680}^{+}. The pH dependence of Tyr_D oxidation kinetics at low temperature could be satisfactorily explained by assuming a single protonatable group with a pK_a of about 7.6 [20]. It has not been determined whether this pK_a corresponds to the hydrogen-bonding partner D2-His189, in support of the first mechanism, or to another proton accepting base in the vicinity of Tyr_D or to Tyr_D itself, in support of the second mechanism.

Ferreira et al. [15] have proposed a structural model for PSII in which a hydrogen-bonding network around Tyr_D involves not only D2-His189 and D2-Gln164, directly interacting with Tyr_D, but also D2-Asn292, D2-Arg294, and Glu364 from the CP47 subunit of PSII. The involvement of other residues in close proximity to Tyr_D should not be overlooked, as we have previously shown that the presence of phosphate and formate at pH 6 alters both the flash yield of Tyr_D oxidation and the stability of $Tyr_D^{\cdot}$, properties similar to those observed at higher pH, without perturbing the IR signature of reduced and oxidized Tyr_D, i.e. the properties of the interactions formed by Tyr_D and D2-His189 (see below) [21,22]. These data suggest that the delocalized hydrogen-bonding network implied by the X-ray structure of PSII [15,17] might play a crucial role in the regulation of $Tyr_D^{\cdot}$ stability [22].

The mechanistic reasons for the pH control of Tyr_D oxidation kinetics and stability are key to understanding the structural factors that tune the kinetic properties of redox-active tyrosines in proteins, a question that we address here using Fourier transform infrared (FTIR) difference spectroscopy.

In contrast with other techniques, FTIR difference spectroscopy provides information on the chemical properties of redox-active tyrosines in both the oxidized and reduced (dark-stable) states [21–27]. IR modes of $Tyr_D^{\cdot}$ and Tyr_D were identified using specific isotope labeling of the tyrosines [25,26]. Two bands at 1503 cm^{-1} and 1250 cm^{-1} were assigned to the ν(C⋯O) mode of $Tyr_D^{\cdot}$ and to the ν(C–O) and/or δ(COH) mode of Tyr_D, respectively [25,26]. We concluded from the analyses of model compounds and of a mutant where D2-His189 was replaced by Gln that: 1) the IR modes are sensitive to the interactions formed by $Tyr_D^{\cdot}$ and Tyr_D with their immediate surroundings, 2) Tyr_D is protonated at pH 6, and 3) both Tyr_D and $Tyr_D^{\cdot}$ in the WT strain are in hydrogen-bonded contact with the neutral imidazole of D2-His189 [24,25,27].

In the present paper, we investigate the pH dependence of the $Tyr_D^{\cdot}$/Tyr_D FTIR difference spectra using WT PSII core complexes isolated from *Synechocystis* sp. PCC 6803 with specifically labeled tyrosines in H_2O and ^2H_2O buffers, and using the D2-Gln164Glu mutant. We show that the protonation state of a residue other than Tyr_D or D2-His189 affects the interaction between reduced Tyr_D and D2-His189.

2. Materials and methods

Mn-depleted PSII core complexes were isolated, according to Tang and Diner [28] followed by the hydroxylapatite step of Rögner et al. [29], from the glucose tolerant [30] and phycocyanin deficient "olive" strain [28] of the cyanobacterium *Synechocystis* sp. PCC 6803. For the specific tyrosine labeling, the cyanobacteria were grown photoautotrophically for 6–7 days in BG-11 medium [31] containing 0.5 mM phenylalanine, 0.25 mM tryptophan, and 0.25 mM isotopically labeled tyrosine [3]. The $^{13}C_1(4)$ and $^{13}C_6$ (98% isotope enriched) were purchased from Cambridge Isotope Laboratories. The glutamine codon at position 164 of the psbD1 gene, encoding the D2 polypeptide, was replaced with that for glutamic acid in the "olive" strain of *Synechocystis* sp. PCC 6803 as described in Tang et al. [12].

2.1. FTIR sample preparation

PSII samples from a concentrated stock (≈5 mg Chl/mL) were washed using Microcon-30 (Millipore) concentrators and suspended in either 50 mM Bis–Tris pH 6.0, Hepes pH 7.0, Tris pH 7.5 or pH 8.5, or Caps pH 10, containing 10 mM NaCl and 5 mM $MgCl_2MgCl_2$ at a final Chl concentration of 6 mg Chl/mL. Approximately 40 μg Chl were used for each FTIR sample. For $H_2O/^2H_2O$ exchange experiments, the buffers in H_2O were dried using a Speed-Vacuum system and resuspended in ^2H_2O. The concentrated PSII sample was washed by dilution in the deuterated buffer at pH 8.5 and subsequent concentration, followed by a second resuspension in the deuterated buffer for 12 h at 8 °C before concentration for the FTIR analysis at pH 8.5.

One microliter of a 0.3 M ferricyanide/0.15 M ferrocyanide solution was deposited on a CaF_2 window. Six microliters of the solution of PSII core complex was also placed on the window and slightly concentrated under a N_2-gas stream. The IR sample was maintained at 4 °C using a circulating cooler (Julabo). The samples were dark-adapted for 4 h before each light-induced reaction. Illumination for 1 s was performed using a 670 nm emitting laser diode (Roithner Lasertechnick, Vienna). The FTIR spectra were recorded for about 3 min (200 scans) before and beginning 2 s after illumination. The spectra were recorded at 4 cm^{-1} resolution using a Bruker IFS 25 FTIR spectrometer equipped with a liquid N_2-cooled MCT-A detector.

3. Results and discussion

3.1. pH dependence of the $Tyr_D^{\cdot}$/Tyr_D FTIR difference spectrum

Fig. 1 shows the $Tyr_D^{\cdot}$/Tyr_D FTIR difference spectra recorded at different pHs between 6 and 10 (spectra A to E) using Mn-depleted PSII samples from *Synechocystis* sp. PCC 6803. In these spectra, the negative bands correspond to the IR modes of the dark-adapted state, before illumination. The positive bands correspond to the light-induced state, where $Tyr_D^{\cdot}$ is formed. The overall appearance of the $Tyr_D^{\cdot}$/Tyr_D FTIR difference spectra is conserved over the whole pH range, with characteristic bands in the amide I region at 1702(−)/1696 (+), 1652(+) and 1644(−) cm^{-1}, and in the amide II region at 1551(+) and 1542(−) cm^{-1} remaining almost unchanged (Fig. 1).

We have previously demonstrated, using tyrosine ^{13}C- and ^2H-labeling, that the positive band at 1503 cm^{-1} corresponds to the ν(C–O) IR mode of $Tyr_D^{\cdot}$[1] [25, see also 26]. Fig. 1 shows that the frequency of this ν(C–O) IR

[1] The ν(C-O) IR mode of $Tyr_D^{\cdot}$ was identified in $Tyr_D^{\cdot}$/Tyr_D FTIR difference spectra recorded at pH 6 in phosphate buffer with formate [25]. We have shown recently that formate does not alter the ν(C-O) mode .frequency and hence the interactions between $Tyr_D^{\cdot}$ and D2-His189 [22].

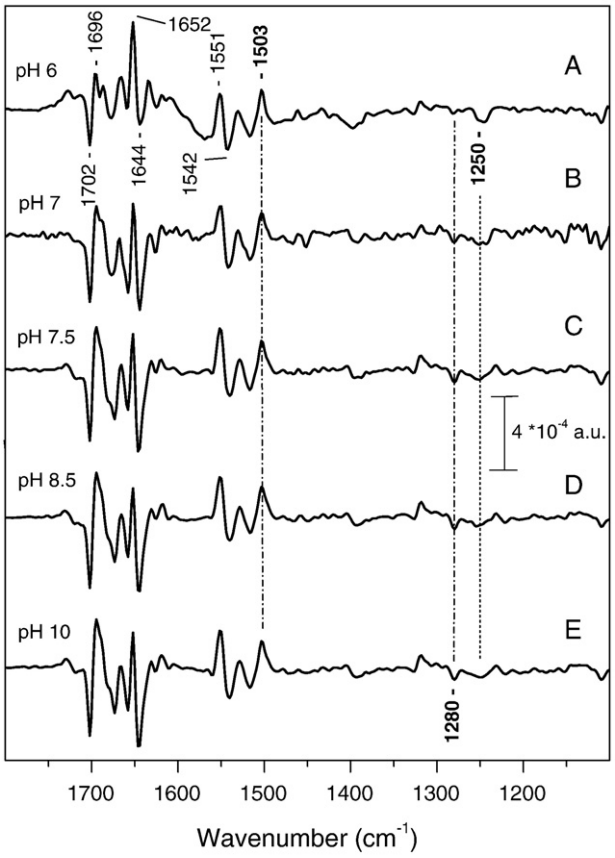

Fig. 1. Tyr_D/Tyr_D FTIR difference spectra recorded using Mn-depleted PSII core complexes of *Synechocystis* sp. PCC 6803 A) in Bis–Tris buffer at pH 6; B) in Hepes buffer pH 7; C) in Tris buffer pH 7.5, and D) pH 8.5; E) in Caps buffer pH 10. The spectra correspond to the average of 10 to 15 light-induced differences taken with two to three samples.

mode remains unchanged throughout the whole range from pH 6 to pH 10. As the frequency of the ν(C–O) IR mode of tyrosine radicals and related model compounds is highly sensitive to hydrogen-bonding interactions, charge distribution, and polarity of the environment [24,25,27 and references therein], this result provides evidence that the interactions between the radical Tyr_D and its hydrogen-bonding partner(s) D2-His189 (and D2-Gln164) remain unchanged over the whole pH range.

The Tyr_D/Tyr_D spectrum at pH 6 (Fig. 1A) was recorded using Bis–Tris buffer. We have shown that in all Tyr_D/Tyr_D FTIR difference spectra recorded at pH 6, with phosphate/formate, or with Mes, or with Bis–Tris buffer, a band at 1250 cm^{-1} is a marker for reduced Tyr_D [22,25, see also 32]. Based on labeling experiments, this band was shown to involve the C_4–O bond of Tyr_D and assigned to the δ(COH) mode [25]. By comparison with IR spectra of cresol in interaction with various chemical groups, we deduced from the frequency of this mode, that Tyr_D is protonated and that it interacts mainly with the neutral side chain of D2-His189 at pH 6 (see below) [25]. Indeed, the D2-His189Gln mutation markedly modified the band pattern of Tyr_D at 1250 cm^{-1}, and the ν(CO) and δ(COH) modes of Tyr_D were assigned at 1267 and 1228 cm^{-1}, respectively in the mutant [25].

Fig. 1 shows that the δ(COH) mode of Tyr_D is also sensitive to the pH. An amplitude decrease was reproducibly observed at 1250 cm^{-1} upon increasing the pH 6 to 8.5. In parallel, another pH sensitive negative band was observed at 1280 cm^{-1} showing an amplitude increase upon increasing the pH from 6 to 8.5 (Fig. 1B, C, D, Fig. 2A). The change in amplitude was largest between pH 6 and 8.5 for both the 1250 and 1280 cm^{-1} signals, and did not evolve further above pH 8.5. At pH 8.5 and above, a negative band is also observed at 1221cm^{-1} in the Tyr_D/Tyr_D spectrum (Fig. 2A).

In order to identify the origin of the 1280-cm^{-1} band, we compared Tyr_D/Tyr_D FTIR spectra recorded at pH 8.5 or pH 10 using unlabeled PSII core complexes (Fig. 3A, B black lines) to those recorded with PSII cores containing tyrosine ^{13}C labeled at all six ring carbons ($^{13}C_6$-Tyr, pH 8.5, Fig. 3A red line) or only at the ring carbon bearing the phenolate oxygen ($^{13}C_1$(4)-Tyr, pH 10, Fig. 3B red line). Upon $^{13}C_6$-Tyr labeling, the 1280 cm^{-1} band shifted to 1247 cm^{-1}. This shift gives rise to a negative band at 1280 cm^{-1} and a positive one at 1246 cm^{-1} in the ^{12}C-minus-$^{13}C_6$ double difference spectrum, in which only the tyrosine IR modes sensitive to Tyr $^{13}C_6$-labeling are expected to contribute (Fig. 4A). The 1280-cm^{-1} band downshifted unambiguously to 1260 cm^{-1} in PSII samples upon $^{13}C_1$(4)-Tyr labeling (Fig. 3B). Accordingly, the ^{12}C-minus-$^{13}C_1$(4) double difference spectrum (Fig. 4B) showed a negative band at 1280 and a positive one at 1262 cm^{-1}. The shifts of the 1280 cm^{-1} band, by − 20 and − 33 cm^{-1} upon tyrosine $^{13}C_1$(4)- and $^{13}C_6$-labeling, respectively, have amplitudes close to those observed previously for the band at 1250 cm^{-1} of Tyr_D at pH 6 (− 24 and − 30 cm^{-1}, respectively, [25]), and the labeling experiments demonstrate the involvement of the tyrosine C_4–O bond in the vibrational band at 1280 cm^{-1}.

We also detected intensity changes at 1250 and ≈1220 cm^{-1} in Fig. 3B which give rise to negative bands at 1250 and 1220 cm^{-1} in the ^{12}C-minus-$^{13}C_1$(4) double difference spectrum (Fig. 4B). The band at 1250 cm^{-1} is assigned to ^{12}C-Tyr_D, and the positive band at 1228 cm^{-1} is assigned to the corresponding mode of $^{13}C_1$(4)-Tyr. Indeed, a downshift from 1250 to 1228 cm^{-1} is totally in agreement with the shift observed for the 1250-cm^{-1} band of Tyr_D in spectra recorded at pH 6 [25]. The bands at 1250 and 1228 cm^{-1} are thus assigned to Tyr_D

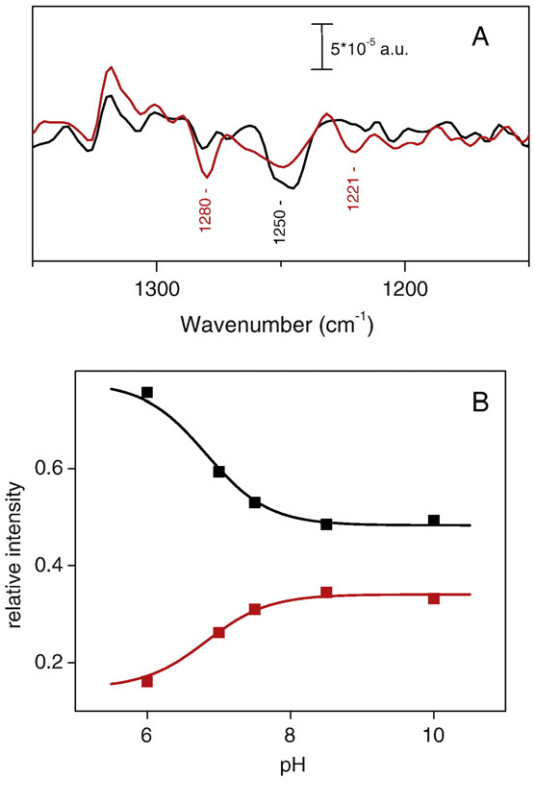

Fig. 2. A) superposition of the Tyr_D/Tyr_D FTIR spectra recorded at pH 6 (black line) and at pH 8.5 (red line) in the 1350–1150 cm^{-1} range; B) pH dependence of the bands at 1280 cm^{-1} (black line) and 1250 cm^{-1} (red line). The relative contribution of the 1280 cm^{-1} band was obtained by calculating the integrals of the curve between 1288 and 1272 cm^{-1} at a given pH and by normalizing it to the integral of amplitudes between 1288 and 1238 cm^{-1}. The relative contribution of the 1250 cm^{-1} was calculated using the integral of the curve between 1260 and 1240 cm^{-1} normalized to the integral between 1288 and 1238 cm^{-1}.

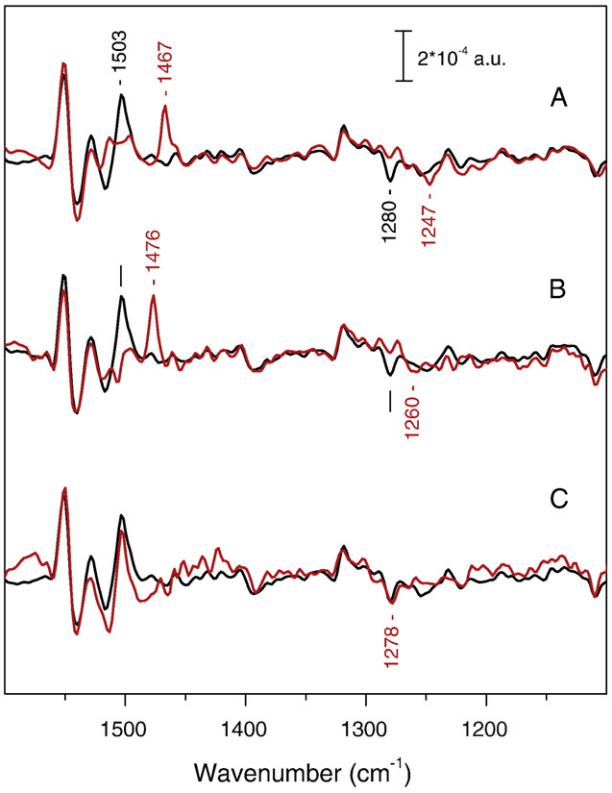

Fig. 3. Superposition of the Tyr_D/Tyr_D FTIR difference spectra recorded with Mn-depleted PS II core of *Synechocystis* sp. PCC 6803 unlabeled in H_2O (black lines at pH 8.5, A and C, or pH 10, B) and A) $^{13}C_6$-labeled tyrosine (red line) in Tris buffer pH 8.5, B) $^{13}C_1$(4)-labeled tyrosine (red line) in caps buffer at pH 10; C) unlabeled tyrosine in ^2H_2O Tris buffer at pH 8.5 (red line).

in a fraction of PSII centers insensitive to the pH change. The third tiny negative band at 1220 cm^{-1} (Fig. 4B) is best interpreted as a band from ^{12}C-Tyr_D. The corresponding positive band expected at lower frequency for $^{13}C_1$(4)-labeled Tyr_D is beyond the detection limit of the experiment. The band at 1220 cm^{-1} is tentatively assigned to a contribution from the Tyr_D C_4–O bond at high pH. The bands at 1250, 1228, and 1220 cm^{-1} were absent in the ^{12}C-minus-$^{13}C_6$ double difference spectrum (Fig. 4A). This is explained by the amplitude of the shift induced by $^{13}C_6$-Tyr labeling, which leads to an overlap between the negative bands of unlabeled Tyr with the positive contributions from $^{13}C_6$-Tyr.

The present data thus show that in PSII from *Synechocystis* sp. PCC 6803, the infrared modes of reduced Tyr_D are pH dependent for a fraction of the PSII centers. The C_4–O bond of reduced Tyr_D is characterized by a negative band at 1250 cm^{-1} at pH 6 and by a band at 1280 cm^{-1} at pH 8.5 and 10. Moreover, if we compare the intensity of the 1280 and 1250 cm^{-1} bands as a function of pH (Fig. 2B), we clearly observe a parallelism between the intensity decrease of the 1250 -cm^{-1} band and the increase in intensity of the 1280 -cm^{-1} band. This effect roughly follows the titration with a single pK_a of ≈7. The apparent pK_a is similar to that corresponding to the ability to rapidly oxidize Tyr_D and to form $Tyr_D^{\cdot}$ at low temperature, as observed by EPR [19,20]. This phenomenon involved approximately 75% of the PSII centers in *Synechocystis* sp. PCC 6803. It is not straightforward to estimate the fraction of PSII centers, in which the IR mode of Tyr_D depends on pH. Indeed, there is a residual negative band at pH 8 at 1250 cm^{-1}, but the band shape is different and part of this band is not sensitive to tyrosine labeling (Fig. 3). From the comparison of the relative intensities of the 1477 and 1250 cm^{-1} bands in the ^{12}C-minus-$^{13}C_1$(4) double difference spectra recorded at pH 6 [25] and at pH 10 (Fig. 4B), we conclude that Tyr_D is sensitive to pH in at least 60% of the PSII centers.

The change as a function of pH observed for reduced Tyr_D contrasts with the absence of any change on the properties of the ν(C–O) mode of the $Tyr_D^{\cdot}$ radical at 1503 cm^{-1}. Moreover, the experiments with labeled tyrosine (Fig. 3A, B) show that the positive band at 1503 cm^{-1} is downshifted to 1467 and 1476 cm^{-1}, upon $^{13}C_6$ and $^{13}C_1$(4)-Tyr labeling, respectively, and that these shifts are almost identical to those measured at pH 6 (to 1468 and 1477 cm^{-1}, respectively, [25]). Since the ν(C–O) mode frequency of $Tyr^{\cdot}$ is highly sensitive to changes in the properties of its environment, and to the presence of D2-His189 [24,25,27], these data show that the hydrogen-bonding interaction formed by $Tyr_D^{\cdot}$ and D2-His189 remains unchanged, whatever the pH. These results are in line with high-field EPR data showing i) that the g_x value of $Tyr_D^{\cdot}$, sensitive to the electrostatic character of the environment, is dominated by the hydrogen-bonding interaction between $Tyr_D^{\cdot}$ and D2-His189, [16,33] and ii) that the g_x frequency of the $Tyr_D^{\cdot}$ radical formed at temperatures higher than 70K is the same for PSII samples at pH 6 or pH 8.7 [33–35]. The FTIR results and the high field EPR data indicate that the side chain of D2-His189 is neutral after $Tyr_D^{\cdot}$ formation over the whole pH range.

Faller et al. studied the properties of the $Tyr_D^{\cdot}$ radical resulting from the oxidation of Tyr_D by P_{680}^{+} at cryogenic temperature (10K) for a fraction of PSII samples at pH 8.7 [34]. The very low g_x value observed for this radical (g=2.00643) was explained by a highly electropositive environment. This radical then relaxed to the usual g_x value with an increase in temperature. The authors interpreted this behavior as the formation of $Tyr_D^{\cdot}$ in interaction with an imidazolium, prior to a thermally activated proton transfer from imidazolium to an unknown proton acceptor. Another possible interpretation was that tyrosinate instead of tyrosine was present at pH 8.7 in strong hydrogen-bonding interaction with the D2-His189 imidazole. In that case, $Tyr_D^{\cdot}$ formation involves an electron transfer only, which is not expected to be blocked at 10K. The low g_x value observed in the high field EPR spectrum recorded at 10K would then reflect the persistence of this strong interaction after $Tyr_D^{\cdot}$ formation, between $Tyr_D^{\cdot}$ and the histidine proton.

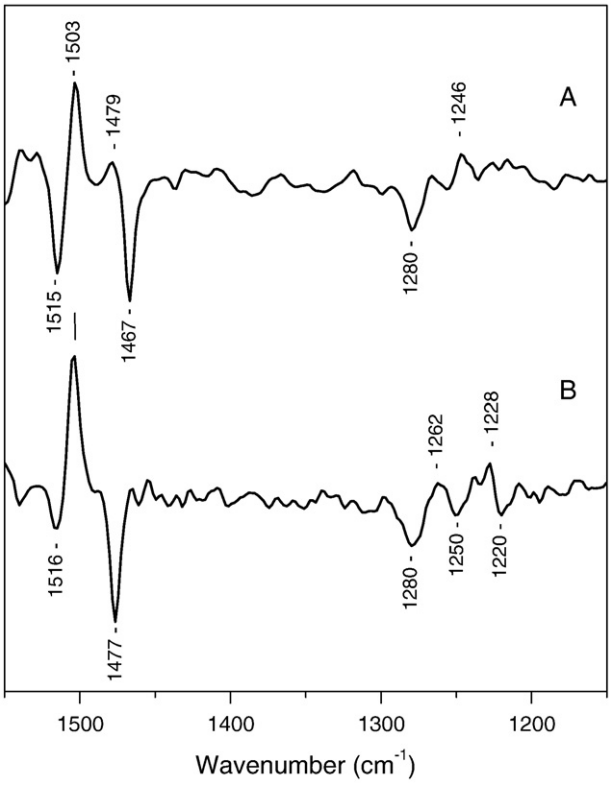

Fig. 4. A)^{12}C-minus-$^{13}C_6$-Tyr and B)^{12}C-minus-$^{13}C_1$(4)-Tyr double difference spectra calculated from spectra of Fig. 3A and B, respectively.

Recovery of the usual g_x value for $Tyr_D^{\cdot}$ at 77K would be due to a thermally activated structural relaxation [34]. For this second interpretation, it is clear that the radical intermediate would be generated only at high pH, because reduced Tyr_D needs to be in the tyrosinate form. In the first case, the impossibility to form the $Tyr_D^{\cdot}$ imidazolium intermediate at pH 6 could be explained by the presence of imidazolium already in the reduced Tyr_D-state. Alternatively, formation of this $Tyr_D^{\cdot}$-imidazolium intermediate could be impaired by electrostatic constraints due to the protonation of another residue. This supposes a difference in charge distribution around the Tyr_D–D2-His189 pair at pH 6 as compared to pH 8.7. It may also indicate that different proton pathways are involved at pH 6 and 8.7 for the proton release from Tyr_D.

The two different mechanisms imply therefore that either Tyr_D deprotonates with a pK_a of about 7.5 in a fraction of the PSII centers from *Synechocystis* sp. PCC 6803 or that the pH-dependent changes in the Tyr_D oxidation kinetics and FTIR difference spectra are due to changes in the Tyr_D environment at D2-His189 or at a greater distance.

3.2. Protonation status of Tyr_D at pH 8.5

The infrared absorption spectra of tyrosine and tyrosinate differ significantly [36, and references therein]. Two intense IR modes can be used as markers of tyrosine deprotonation, the ν(CO) mode and the ν_{19}(CC) ring mode. The ν(CO) mode is not only sensitive to the protonation state of Tyr but also to hydrogen-bonding interactions, with large changes depending on the nature of the hydrogen-bonding partner [25,37].

The intense ν_{19}(CC) IR mode is reported at 1518 cm^{-1} for tyrosine and at 1500–1499 cm^{-1} for tyrosinate in solution [36,37]. At pH 6, we identified the ν_{19}(CC) IR mode of reduced Tyr_D at 1513–1511 cm^{-1} in the ^{12}C-minus-$^{13}C_6$ and ^{12}C-minus-$^{13}C_1$(4) double difference spectra calculated from the $Tyr_D^{\cdot}/Tyr_D$ spectra recorded with unlabelled and Tyr-labeled PSII [25]. In the 1550–1400 cm^{-1} region, the ^{12}C-minus-$^{13}C_6$ double difference spectrum calculated for PSII samples at pH 8.5 (Fig. 4A) is very similar to that calculated for samples at pH 6. A negative band is clearly detected at 1515 cm^{-1}, downshifted to 1479 cm^{-1} upon $^{13}C_6$-labeling. This band is typical of a protonated tyrosine. In contrast, no negative band appears at ≈1498 cm^{-1} that could account for the ν_{19} (CC) mode of tyrosinate in a fraction of the PSII centers. The same conclusion can be drawn from the inspection of the ^{12}C-minus-$^{13}C_1$(4) difference spectrum (Fig. 4B), where the ν_{19}(CC) mode is clearly detected at 1516 cm^{-1}. Therefore, we conclude that Tyr_D remains protonated in the whole range from pH 6 to pH 10. The slight change in the ν_{19}(CC) mode frequency with pH and the spectral changes in the 1300–1200 cm^{-1} region reveal changes in interactions between reduced Tyr_D and its environment. The lack of large overall change in the $Tyr_D^{\cdot}/Tyr_D$ FTIR spectra recorded at different pHs suggests that these changes involve minute structural reorganization.

3.3. Origin of the spectral change of Tyr_D in the 1300–1200 cm^{-1} region

For (protonated) tyrosine, the main ν(CO) mode is observed at 1248–1250 cm^{-1} in solution [25,26,36], with shifts of − 25 and − 22 cm^{-1}, upon $^{13}C_6$ and $^{13}C_1$(4)-labeling, respectively [25,26]. Actually, both ν(CO) and δ(COH) modes are expected to contribute in the 1280–1100 cm^{-1} range. These modes appear at 1255 and 1175 cm^{-1} for *p*-cresol (the model of Tyr side chain) in the apolar and aprotic solvent CCl_4, i.e. for *p*-cresol free from hydrogen-bonding interactions [38]. The frequency and intensity of these two modes are sensitive to the hydrogen-bonding status of *p*-cresol. In pyridine, i.e. for *p*-cresol forming a hydrogen bond with the pyridine nitrogen, these modes were assigned to 1268 and 1248 cm^{-1}, respectively, based on experiments with deuterated *p*-cresol [25]: while the ν(CO) mode is only slightly downshifted upon H/^{2}H exchange, the δ(COH) mode experiences a large downshift, below 1000 cm^{-1} [25,39]. We previously recorded the absorption spectrum of *p*-cresol in 4(5)-methylimidazole [25] and assigned the ν(CO) and δ(COH) modes to 1271 and 1251 cm^{-1}, respectively, by comparison with the data recorded in pyridine. These modes were assigned at 1269 and 1251 cm^{-1} for *p*-cresol in neutral 1-methylimidazole (1-MeImH) and at 1263 and 1229 cm^{-1}, respectively, for *p*-cresol in 1-methylimidazolium (1-$MeImH_2^+$) [25]. While 4(5)-methylimidazole or 1-MeImH can act as H-bond acceptor or donor; 1-$MeImH_2^+$ only acts as a proton donor to *p*-cresol. This interaction greatly affected the frequency and relative intensity of the two IR modes of *p*-cresol.

For Tyr_D at pH 6, two bands were identified at 1275 and 1250 cm^{-1}, using tyrosine labeling, which we assigned to the ν(CO) and δ(COH) modes, respectively[2]. The close resemblance of these band frequencies and intensities with those of *p*-cresol in 4(5)-methylimidazole was taken as evidence for a main interaction of Tyr_D as a hydrogen bond donor to the neutral imidazole side chain of D2-His189 at pH 6. These data did not support an interaction between Tyr_D and the imidazolium form of D2-His189, consistent with the lack of an intense ν(CC) mode characteristic of imidazolium at 1630 cm^{-1} using ^{13}C-His labeled PSII samples [25]. A very recent DFT analysis of hydrogen-bonded complexes of *p*-cresol by Takahashi and Noguchi [40] predicts slight differences in the IR signature for the COH group of *p*-cresol in a *p*-cresol–4(5)-methylimidazole complex, depending on whether *p*-cresol is acting as a hydrogen donor only, or whether it is also a weak proton acceptor. According to their normal mode predictions, the IR frequencies observed for Tyr_D could be interpreted by a situation where Tyr_D acts as a hydrogen bond donor to the neutral side chain of D2-His189 but also as a weak hydrogen acceptor from another residue in the vicinity of Tyr_D [40]. For such a donor/acceptor form, the mode composition of the IR bands is altered and the bands at 1275 and 1250 cm^{-1} would correspond to the δ(COH) and ν(CO) modes respectively [40].

At pH 8.5 and 10, the IR bands of Tyr_D are altered and the main band is observed at 1280 cm^{-1}. This band is downshifted by 2 cm^{-1} in the $Tyr_D^{\cdot}/Tyr_D$ FTIR difference spectrum recorded at pH 8.5 in ^2H_2O buffer (Fig. 3C). This shift is in agreement with an assignment of this band to the ν(CO) mode of Tyr_D [41][3]. Takahashi et al. [41] performed calculations on the ν(CO) and δ(COH) modes of cresol hydrogen bonding to a series of amide derivatives and concluded that the ν(CO) mode frequency increased with the strength of the hydrogen bond, with frequencies varying from 1266 cm^{-1} up to 1276 cm^{-1}, for *p*-cresol interacting solely as H-bond donor to the amide C = O, without interaction with the primary amine group. Further calculations of the IR mode frequencies for pure H donating *p*-cresol predicted the ν(CO) mode frequency at 1277 cm^{-1} upon interaction with methylimidazole and up to 1279 cm^{-1} upon interaction with methylamine [40]. In these calculations, the frequency and intensity of the δ(COH) mode largely differ depending on the nature of the hydrogen accepting group, with frequencies at 1242 cm^{-1} for 4(5)-methylimidazole, 1254 cm^{-1} for methylamine, or at 1219–1235 cm^{-1} for the oxygen of water, or amide groups [40].

The high frequency and intensity of the ν(CO) mode of reduced Tyr_D at pH greater than 7.5 thus indicate that Tyr_D is involved as a proton donor only in a very strong hydrogen bond. The negative band detected at 1220 cm^{-1} in the 12C-minus-$^{13}C_1$(4) difference spectrum recorded at pH 10 may be assigned to the δ(COH) mode of Tyr_D, suggesting that Tyr_D is not interacting with D2-His189 but with another residue at this pH. This assignment remains however tentative and we cannot exclude that the strong hydrogen-bonding interaction involves D2-His189 side chain.

In addition to D2-His189, the D2-Gln164 side chain is likely at hydrogen-bonding distance from Tyr_D, either directly or indirectly, through a water molecule [15,17]. Indeed, a water molecule was recently proposed to interact directly with Tyr_D [32]. To analyze the

[2] The 1275 cm^{-1} band is very weak and was only detected in ^{12}C-minus-$^{13}C_6$ or ^{12}C-minus-$^{13}C_1$(4) double difference spectra [25].

[3] Although it is difficult to obtain 100% H/^{2}H exchange, we could conclude from the absorption spectrum of the sample that more than 50 % of the peptide amide protons were exchanged (not shown).

influence of the D2-Gln164 on the vibrational properties of Tyr_D, we recorded the $Tyr_D^{\cdot}/Tyr_D$ FTIR difference spectrum in the D2-Gln164Glu mutant at pH 6 and pH 8.5 (Fig. 5). At both pH 6 and 8.5, the side chain of Glu is expected to be in the deprotonated carboxylate form. Under these conditions, one might expect a strong interaction between the COH group of Tyr_D and the carboxylate group of Glu, instead of the interaction with the imidazole side chain of D2-His189.

In the $Tyr_D^{\cdot}/Tyr_D$ spectrum recorded with the D2-Gln164Glu mutant at pH 6 (Fig. 5A red line), spectral changes are observed in the 1300–1200 cm^{-1} region, which are close to those detected with WT PSII at pH 8.5 and above. Indeed, a clear negative band appears at 1280 cm^{-1}, while the intensity of the 1250 cm^{-1} band is weaker than in WT PSII (Fig. 5A). Other changes were detected in the $Tyr_D^{\cdot}/Tyr_D$ FTIR spectrum, at 1407/1386 and at 1566 cm^{-1}, which are best interpreted as a contribution from the carboxylate side chain of D2-Glu164, affected by the formation of the $Tyr_D^{\cdot}$ radical. These data are consistent with the formation of a strong hydrogen-bonding interaction between the phenol group of Tyr_D and the carboxylate side chain of D2-Glu164 in the mutant. They also indicate that the carboxylate group of D2-Glu164 is not the proton acceptor upon $Tyr_D^{\cdot}$ radical formation. The $Tyr_D^{\cdot}/Tyr_D$ spectrum recorded with the D2-Gln164Glu mutant was not markedly modified at pH 8.5, relative to pH 6, in the 1280–1200 cm^{-1} range (Fig. 5B). Finally, the frequency of the ν(CO) mode of Tyr_D was also slightly different in the mutant, at 1504 (pH 6) or 1505 (pH 8.5) cm^{-1} instead of 1503 cm^{-1} in WT PSII, possibly due to the presence of the negative charge in proximity to the Tyr_D CO group.

The experiments performed with the D2-Gln164Glu mutant show that the interactions between Tyr_D and D2-His189 can be modulated at pH 6 by the properties of the residue at position D2-164. The electronegative character of D2-Glu164 may reorient the hydrogen bond formed by Tyr_D towards the Glu side chain rather than toward D2-His189. Alternatively, a strong and exclusive hydrogen-bonding interaction may be formed by Tyr_D with the side chain of D2-His189 as a consequence of a change in the hydrogen-bonding network around D2-Glu164 in the mutant.

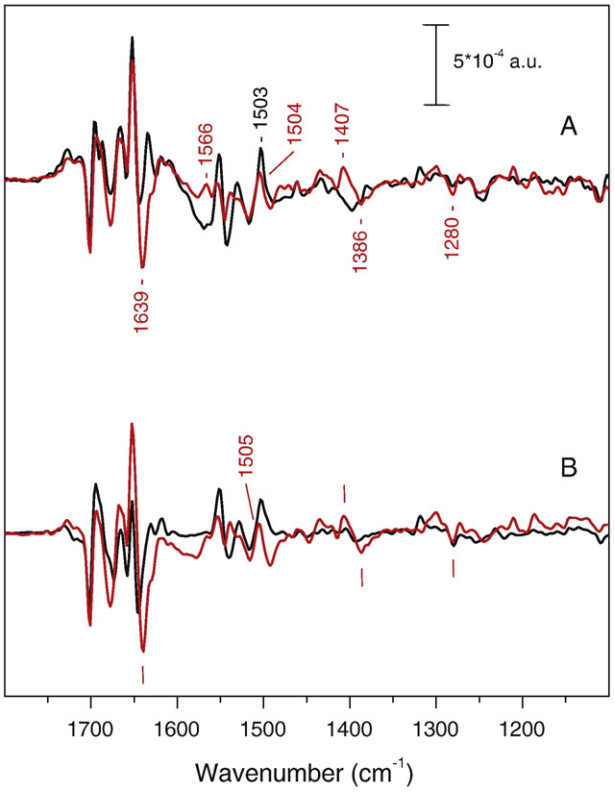

Fig. 5. Superposition of the $Tyr_D^{\cdot}/Tyr_D$ FTIR difference spectra recorded with the D2-Gln164Glu mutant (red line) and WT PSII (black line) A) using Bis–Tris buffer at pH 6, B) using Tris buffer at pH 8.5.

In WT PSII, the effect of pH observed on the IR bands of reduced Tyr_D may result from a change in the (direct or indirect) interaction between the Tyr_D phenol and the side chain of D2-Gln164. The glutamine side chain cannot undergo changes in protonation state over the pH range examined. Thus changes in the properties of another protonatable group, in interaction with D2-Gln164 and/or D2-His189 must be responsible for the changes in the Tyr_D environment as a function of pH. A large hydrogen-bonding network around Tyr_D involves not only D2-His189 and D2-Gln164, but also D2-Asn292, D2-Arg294, and Glu364 from the CP47 subunit of PSII [15]. D2-Arg294 is within hydrogen-bonding distance of D2-His189. Two hydrogen-bonded water molecules sensitive to Tyr_D oxidation, recently identified using ^{18}O-labeled H_2O, must also participate in the hydrogen-bonding network [32]. Protonatable residues CP47-Glu364 and D2-Arg294 and the water molecules may be responsible for the effect of pH in Tyr_D, by modulating the properties of the Tyr_D–D2-His189 interaction.

We have previously observed that treatment with phosphate and formate destabilizes $Tyr_D^{\cdot}$ at pH 6 [25]. Using ^{13}C-labeled formate we demonstrated that formate binds in PSII in the Tyr_D state at pH 6 [22]. Comparison of $Tyr_D^{\cdot}/Tyr_D$ spectra recorded with or without formate showed, however, that the IR bands of reduced Tyr_D were not directly affected by the presence of formate. In contrast, binding of formate modified the FTIR difference spectra at 1676/1690 cm^{-1}, suggesting a possible interaction with an arginine side chain. This effect was not observed with the larger anion acetate [22]. We proposed that formate binding at D2-Arg294, could perturb protonation reactions associated with the oxidation/reduction of Tyr_D. The direct effect of pH on the properties of the Tyr_D COH group and the effect of formate binding, at some distance from Tyr_D point two different mechanisms that regulate the properties of redox-active Tyr_D.

3.4. Conclusions

We conclude, using FTIR difference spectroscopy, that the reduced but not the oxidized form of Tyr_D undergoes changes in its hydrogen-bonded interaction with its immediate environment between pH 6 and 10. The FTIR data also clearly show that reduced Tyr_D remains protonated in the pH range examined in this work. Thus, the fast oxidation kinetics of Tyr_D and the ability to oxidize it at low temperature at pH>7.5 are not the consequence of a pure electron transfer reaction produced by prior formation of tyrosinate at these pHs. The FTIR data also do not support a change in the protonation state of the D2-His189 side chain from imidazolium (pH 6) to imidazole (pH>7.5) in the reduced Tyr_D state.

At pH greater than 7.5, Tyr_D is characterized by a ν(CO) mode at 1280 cm^{-1}, indicating that it is involved in a very strong hydrogen bond, as a H-bond donor only, while at pH 6, Tyr_D acts mainly as a weaker H-bond donor to the D2-His189 side chain and possibly as a weak H-bond acceptor. The changes in the FTIR mode frequencies of Tyr_D at high pH could correspond to the formation of a stronger and exclusive hydrogen-bonding interaction with the neutral side chain of D2-His189 (possibly with the disappearance of a weak donating hydrogen bond to Tyr_D), or to an interaction with another residue. A stronger interaction with D2-His189 could be the result of an increased electronegative character of the imidazole side chain.

The FTIR data point to the role of a protonatable group (with a pK_a of ≈7) other than D2-His189, in modifying the characteristics of the Tyr_D hydrogen-bonding interactions. Given the large hydrogen-bonding network described around Tyr_D, and the fact that the pH-induced changes concern only a fraction of the PSII centers, this phenomenon may result from a charge delocalized on more than one residue. In this respect, it is important to stress the possible role of

water molecules sensitive to the formation of the Tyr_D radical, one of these possibly directly interacting with Tyr_D [32].

The involvement of Tyr_D in a strong hydrogen-bonding interaction correlates with the ability to rapidly oxidize Tyr_D, and to oxidize it at cryogenic temperature [19,20]. This correlation suggests that a strong hydrogen-bonding interaction could be at the origin of the very low g_x (g=2.00643) value observed for the Tyr_D radical formed at cryogenic temperature on PSII samples at pH 8.7 [34]. Since the properties of the relaxed Tyr_D radical are the same in the whole pH range, the formation of a strong hydrogen-bonding interaction between Tyr_D and a residue other than D2-His189 at pH greater than 7 would imply that a structural relaxation occurs after Tyr_D oxidation resulting in the establishment of the Tyr_D–D2-His189 hydrogen-bonding interaction as indicated by ENDOR [12,14].

If the ability to oxidize Tyr_D efficiently correlates with a privileged orientation of the Tyr_D phenolic proton towards D2-164Gln or a residue other than D2-His189 at pH>7, then D2-His189 may not be directly involved (as an intermediate) in the proton transfer associated with Tyr_D oxidation. Instead its main role would be to structure a hydrogen-bonding network, necessary for rapid proton transfer to another residue and, following the electron and proton transfer, as a hydrogen bond donor to Tyr_D.

Acknowledgements

A. Boussac and J. Lavergne are gratefully acknowledged for their useful discussions. B.A.D. gratefully acknowledges the support of the National Research Initiative of the USDA Cooperative State Research, Education and Extension Service (grant No. 2003–35318–13589).

References

[1] J. Stubbe, W. A. van der Donk, Protein radicals in enzyme catalysis, Chem. Rev. 98 (1998) 705–762 and 2661–2662.
[2] G. Backes, M. Sahlin, B.M. Sjöberg, T.M. Loehr, J. Sanders-Loehr, Resonance Raman spectroscopy of ribonucleotide reductase. Evidence for a deprotonated tyrosyl radical and photochemistry of the binuclear iron center, Biochemistry 28 (1989) 1923–1929.
[3] B.A. Barry, G.T. Babcock, Tyrosine radicals are involved in the photosynthetic oxygen-evolving system, Proc. Natl. Acad. Sci. U. S. A. 84 (1987) 7099–7103.
[4] K. Budiman, A. Kannt, S. Lyubenova, O.M.H. Richter, B. Ludwig, H. Michel, F. MacMillan, Tyrosine 167: the origin of the radical species observed in the reaction of cytochrome *c* oxidase with hydrogen peroxide in *Paracoccus denitrificans*, Biochemistry 43 (2004) 11709–11716.
[5] A. Ivancich, H.M. Jouve, B. Sartor, J. Gaillard, EPR investigation of compound I in *Proteus mirabilis* and bovine liver catalases: formation of porphyrin and tyrosyl radical intermediates, Biochemistry 36 (1997) 9356–9364.
[6] A. Ivancich, P. Dorlet, D.B. Goodin, S. Un, Multifrequency highfield EPR study of the tryptophanyl and tyrosyl radical intermediates in wild-type and the W191G mutant of cytochrome *c* peroxidase, J. Am. Chem. Soc. 123 (2001) 5050–5058.
[7] S. Chouchane, S. Girotto, S. Yu, R.S. Magliozzo, Identification and characterization of tyrosyl radical formation in *Mycobacterium tuberculosis* catalase-peroxidase (KatG), J. Biol. Chem. 277 (2002) 42633–42638.
[8] C. Aubert, P. Mathis, A.P. Eker, K. Brettel, Intraprotein electron transfer between tyrosine and tryptophan in DNA photolyase from *Anacystis nidulans*, Proc. Natl. Acad. Sci. U. S. A. 96 (1999) 5423–5427.
[9] B.A. Diner, R.D. Britt, The redox-active tyrosines y_z and y_d. In photosystem II: the light-driven water: plastoquinone oxidoreductase, in: WydrzynskiT.J. , SatohK. (Eds.), Advances in Photosynthesis and Respiration, vol. 22, Springer, Dordrecht, 2005, pp. 207–233.
[10] A.W. Rutherford, A. Boussac, P. Faller, The stable tyrosyl radical in photosystem II: why D? Biochim. Biophys. Acta 1655 (2004) 222–230.
[11] G.M. Ananyev, I. Sakiyan, B.A. Diner, G.C. Dismukes, A functional role for tyrosine-D in assembly of the inorganic core of the water oxidase complex of photosystem II and the kinetics of water oxidation, Biochemistry 41 (2002) 974–980.
[12] X.-S. Tang, D.A. Chisholm, G.C. Dismukes, G.W. Brudwig, B.A. Diner, Spectroscopic evidence from site-directed mutants of *Synechocystis* PCC6803 in favor of a close interaction between histidine 189 and redox-active tyrosine 160, both of polypeptide D2 of the photosystem II reaction center, Biochemistry 32 (1993) 13742–13748.
[13] C. Tommos, L. Davidson, B. Svensson, C. Madsen, W.F.J. Vermaas, S. Styring, Modified EPR spectra of the tyrosineD radical in photosystem II in site-directed mutants of *Synechocystis* sp. PCC 6803: identification of side chains in the immediate vicinity of tyrosineD on the D2 protein, Biochemistry 32 (1993) 5436–5441.
[14] K.A. Campbell, J.M. Peloquin, B.A. Diner, X.S. Tang, D.A. Chisholm, R.D. Britt, The *t*-nitrogen of D2 histidine 189 is the hydrogen bond donor to the tyrosine radical Y_D of photosystem II, J. Am. Chem. Soc. 119 (1997) 4787–4788.
[15] K.N. Ferreira, T.M. Iverson, K. Maghlaoui, J. Barber, S. Iwata, Architecture of the photosynthetic oxygen-evolving center, Science 303 (2004) 1831–1838.
[16] S. Un, A. Boussac, M. Sugiura, Characterization of the tyrosine-Z radical and its environment in the spin-coupled S_2Tyr_Z state of photosystem II, Biochemistry 46 (2007) 3138–3150.
[17] B. Loll, J. Kern, W. Saenger, A. Zouni, J. Biesiadka, Towards complete cofactor arrangement in the 3.0Å resolution structure of photosystem II, Nature 438 (2005) 1040–1044.
[18] A. Boussac, A.-L. Etienne, Oxido-reduction kinetics of Signal II slow in tris-washed chloroplasts, Biochem. Biophys. Res. Commun. 109 (1982) 1200–1205.
[19] P. Faller, R.J. Debus, K. Brettel, M. Sugiura, A.W. Rutherford, A. Boussac, Rapid formation of the stable tyrosyl radical in photosystem II, Proc. Natl. Acad. Sci. U. S. A. 98 (2001) 14368–14373.
[20] P. Faller, A.W. Rutherford, R.J. Debus, Tyrosine D oxidation at cryogenic temperature in photosystem II, Biochemistry 41 (2002) 12914–12920.
[21] R. Hienerwadel, A. Boussac, J. Breton, C. Berthomieu, Fourier transform infrared difference study of tyrosineD oxidation and plastoquinone QA reduction in photosystem II, Biochemistry 35 (1996) 115447–115460.
[22] R. Hienerwadel, S. Gourion-Arsiquaud, R. Bassi, B.A. Diner, C. Berthomieu, Formate binding near the redox-active $tyrosine_D$ in photosystem II: consequences on the properties of Tyr_D, Photosynth. Res. 84 (2005) 139–144.
[23] T. Noguchi, C. Berthomieu, Photosystem II: the light-driven water plastoquinone oxidoreductase, in: WydrzynskiT.J. , SatohK. (Eds.), Chap 16, Molecular Analysis by Vibrational Spectroscopy, in Advances in Photosynthesis and Respiration Series Vol 22, Springer, 2005, pp. 367–387.
[24] C. Berthomieu, R. Hienerwadel, Vibrational spectroscopy to study the properties of redox-active tyrosines in photosystem II and other proteins, Biochim. Biophys. Acta 1707 (2005) 51–66.
[25] R. Hienerwadel, A. Boussac, J. Breton, B.A. Diner, C. Berthomieu, Fourier transform infrared difference spectroscopy of photosystem II tyrosine D using site-directed mutagenesis and specific isotope labeling, Biochemistry 36 (1997) 14712–14723.
[26] T. Noguchi, Y. Inoue, X.S. Tang, Structural coupling between the oxygen-evolving Mn cluster and a tyrosine residue in photosystem II as revealed by Fourier transform infrared spectroscopy, Biochemistry 36 (1997) 14705–14711.
[27] C. Berthomieu, R. Hienerwadel, A. Boussac, J. Breton, B.A. Diner, Hydrogen bonding of redox-active tyrosine Z of photosystem II probed by FTIR difference spectroscopy, Biochemistry 37 (1998) 10547–10554.
[28] X.-S. Tang, B.A. Diner, Biochemical and spectroscopic characterization of a new oxygen-evolving photosystem II core complex from the cyanobacterium *Synechocystis* PCC 6803, Biochemistry 33 (1994) 4594–4603.
[29] M. Rögner, P.J. Nixon, B.A. Diner, Purification and characterization of photosystem I and photosystem II core complexes from wild-type and phycocyanin-deficient strains of the cyanobacterium *Synechocystis* PCC 6803, J. Biol. Chem. 265 (1990) 6189–6196.
[30] J.G.K. Williams, Construction of specific mutations in photosystem II photosynthetic reaction centers by genetic engineering methods in *Synechocystis* 6803, Methods Enzymol. 167 (1988) 766–778.
[31] R. Rippka, J. Deruelles, J.B. Waterbury, M. Herdman, R.Y. Stanier, Generic assignments, strain histories and properties of pure cultures of cyanobacteria, J. Gen. Microbiol. 111 (1979) 1–61.
[32] R. Takahashi, M. Sugiura, T. Noguchi, Water molecules coupled to the redox-active tyrosine Y(D) in photosystem II as detected by FTIR spectroscopy, Biochemistry (2007) in press.
[33] S. Un, X.-S. Tang, B.A. Diner, 245GHz high-field EPR study of tyrosine-D° and tyrosine-Z° in mutants of photosystem II, Biochemistry 35 (1996) 679–684.
[34] P. Faller, C. Goussias, A.W. Rutherford, S. Un, Resolving intermediates in biological proton-coupled electron transfer: a tyrosyl radical prior to proton movement, Proc. Natl. Acad. Sci. U. S. A. 100 (2003) 8732–8735.
[35] P. Dorlet, A.W. Rutherford, S. Un, Orientation of the tyrosyl D, pheophytin anion and semiquinone Q_A^- radicals in photosystem II determined by high field electron paramagnetic resonance, Biochemistry 39 (2000) 7826–7834.
[36] G. Dollinger, L. Eisenstein, S.L. Lin, K. Nakanishi, J. Termini, Fourier transform infrared difference spectroscopy of bacteriorhodopsin and its photoproducts regenerated with deuterated tyrosine, Biochemistry 25 (1986) 6524–6533.
[37] C. Berthomieu, C. Boullais, J.M. Neumann, A. Boussac, Effect of ^{13}C-, ^{18}O-, and ^{2}H-labeling on the infrared modes of UV induced phenoxyl radicals, Biochim. Biophys. Acta 1365 (1998) 112–116.
[38] R.J. Jakobsen, The vibrational spectra of *p*-cresol, Spectrochim. Acta 21 (1965) 433–442.
[39] H. Takeuchi, N. Watanabe, I. Harada, Vibrational spectra and normal coordinate analysis of *p*-cresol and its deuterated analogs, Spectrochim. Acta 44 (1988) 749–761.
[40] R. Takahashi, T. Noguchi, Criteria for determining the hydrogen-bond structures of a tyrosine side chain by Fourier transform infrared spectroscopy: density functional theory analyses of model hydrogen-bonded complexes of *p*-cresol, J. Phys. Chem. B in the press.
[41] R. Takahashi, K. Okajima, H. Suzuki, H. Nakamura, M. Ikeuchi, T. Noguchi, FTIR study on the hydrogen bond structure of a key tyrosine residue in the flavin-binding blue light sensor TePixD from *Thermosynechococcus elongatus*, Biochemistry 46 (2007) 6459–6467.